Monolithic diamond Raman laser

Sean Reilly*, Vasili G Savitski, Hangyu Liu, Erdan Gu, Martin D Dawson, and Alan J Kemp

Institute of Photonics, Department of Physics, SUPA, University of Strathclyde, 106 Rottenrow, Glasgow G4 0NW, UK
**Corresponding author: s.reilly@strath.ac.uk*

Received Month X, XXXX; revised Month X, XXXX; accepted Month X, XXXX; posted Month X, XXXX (Doc. ID XXXXX); published Month X, XXXX

A monolithic diamond Raman laser is reported. It utilizes a 13mm radius of curvature lens etched onto the diamond surface and dielectric mirror coatings to form a stable resonator. The performance is compared to that of a monolithic diamond Raman laser operating in a plane-plane cavity. On pumping with a compact Q-switched laser at 532nm (16µJ pulse energy; 1.5ns pulse duration; 10kHz repetition-rate; M^2 <1.5), laser action was observed at the first, second and third Stokes wavelengths (573nm, 620nm and 676nm respectively) in both cases. For the microlens cavity, a conversion efficiency of 84% was achieved from the pump to the total output power, with a slope efficiency of 88%. This compares to a conversion efficiency of 59%, and a slope efficiency of 74% for the plane-plane case. Total Raman output powers of 134mW and 96mW were achieved for the micro-lens and plane-plane cavities respectively.

Recent advances in diamond growth [1] have allowed laser engineers to exploit the material's unrivalled thermo-mechanical properties and large Raman gain coefficient [2]. This has enabled, for example, demonstrations of high average power continuous wave [3], [4] and pulsed [5]–[7] diamond Raman lasers at hard to reach, but commercially significant, wavelengths from the ultraviolet to the mid-infrared [8], [9]. The yellow-orange spectral region is of particular interest, with applications in ophthalmology [10], [11]; however there are few simple, robust and compact yellow orange lasers available.

In this letter, the feasibility of compact and robust monolithic diamond Raman lasers is demonstrated and the performance characteristics are reported. A comparison is drawn between a 2mm long device that uses a microlens structure to form a stable cavity and a 1.6mm long plane-plane resonator. Conversion efficiencies of 84% and 59%, respectively, are achieved despite modest pump pulse energies of <20µJ. These efficiencies are comparable to the 64% reported in a conventional diamond Raman laser pumped at millijoule levels [12].

The single crystal synthetic diamond used to achieve these results was grown using chemical vapour deposition by Element 6 Ltd. Its birefringence was $<1x10^{-6}$ and it had a specified absorption coefficient of $<0.005cm^{-1}$ at 1064nm. The sample used for the plane-plane resonator was $3.6x2x1.6mm^3$, while that used for the micro-lens cavity was $4x4x2mm^3$.

Microlens structures were created on the latter sample using a multi-layer "resist-reflow" process, based on [13], followed by an inductively coupled plasma etch using Ar/Cl_2. An Ar/Cl_2 plasma etch was chosen over more conventional Ar/O_2 recipes because the low etch selectivity between diamond and photoresist enabled the fabrication of micro-lenses with a larger radius of curvature. An array of 8x8 spherical micro-lenses with a diameter of approximately 400µm and radii of curvature of around 13mm were etched on one of the $4x4mm^2$ surfaces. This is a relatively long radius of curvature for a microlens fabricated by resist-reflow on diamond, and was chosen to provide the largest possible cavity mode area, hence reducing the risk of coating damage in the microlens sample.

The back surfaces of both diamonds were coated for high-reflection (HR) at 532nm, to double pass the pump, and partial reflection (PR) at the first Raman shifted wavelength of 573nm (70% reflectivity). The front surfaces were coated for high-transmission (HT) at the pump wavelength (~20% reflectivity) and HR coated at 573nm.

These coated samples were tested in the experimental setup shown in Figure 1 and Figure 2. Both were pumped with an Elforlight SPOT laser emitting Q-switched pulses at 532nm with pulse durations of 1.5ns (full width at half

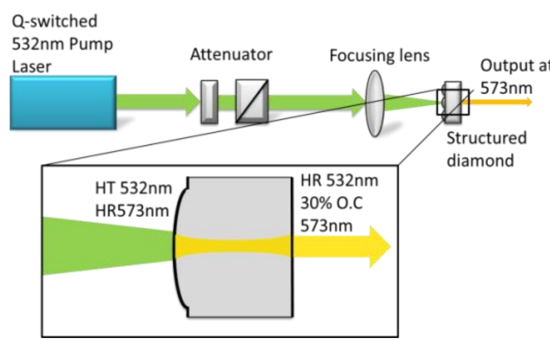

Figure 1. Experimental setup used to achieve Raman laser action in microlens and plane-plane diamond. HT: high transmission; HR: high reflectivity; O.C.: output coupling.

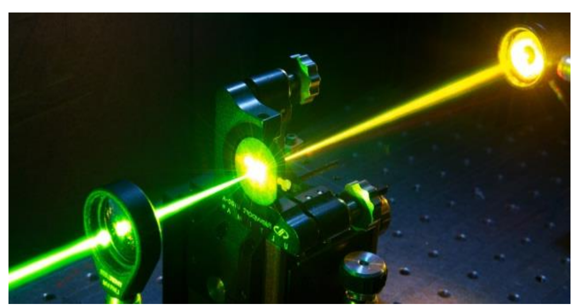

Figure 2. Green to yellow/orange conversion using a monolithic diamond Raman resonator. The photograph was taken at maximum pump power with all three Stokes orders present.

maximum, FWHM) and pulse repetition rates between 1kHz and 10kHz. The results presented in this paper were all taken at 10kHz; however, comparable conversion efficiencies were observed at 1kHz.

The pump was attenuated using a combination of a half wave-plate and a polarizing cube. It was then focused using a 50mm focal length lens. In the case of the microlens sample, it was focused through a single microlens structure onto the back surface of the diamond. This resulted in a pump spot radius of 9µm, which was found to provide slightly better performance than a pump spot size of 18µm. The microlens cavity had a fundamental mode radius of 24µm. Pump light propagated along a <110> direction in the diamond, and was polarized along a <100> direction in the micro-lens case, whilst in the plane-plane system, pump light propagated along a <100> direction and was polarized along a <110> direction.

This set-up resulted in Raman conversion of the green pump at 532nm to the yellow at 573nm when the pump pulse energy reached 1.5µJ for the micro-lens case and 3.7 µJ for the plane-plane case. The pump energies quoted are corrected for the 20% reflectivity of the front coating on both diamonds. The reflectivities at the 2nd Stokes wavelength (620nm) of the coatings deposited on the back and front surfaces of the diamonds were 50% and 40%, respectively. Even with this relatively high combined output coupling of 80% per round trip, a significant fraction of the pump power was converted to the 2nd Stokes wavelength: 59% and 25%, respectively, for the microlens and plane-plane cases at maximum pump power (blue triangles in Figure 3a and Figure 3b). A small amount of 3rd Stokes emission was also present as the pump pulse energy reached maximum (red circles in Figure 3a and Figure 3b). Clamping of the 1st Stokes (green squares in Figure 3a) is observed for the microlens resonator when the 2nd Stokes rises above threshold, but not in the plane-plane case (green squares in Figure 3b). In the case of the microlens cavity, the pre-defined cavity mode confines the 1st Stokes, allowing the 2nd Stokes to efficiently extract energy. In the plane-plane cavity, however, the cavity mode is less restricted, hence potentially less conducive to efficient 2nd Stokes generation. These power transfer curves were measured using a set of calibrated filters. The output at 620nm was measured in both the forward and backward (towards the pump) directions, as backward emission contributed a significant fraction of the total power in this case. Output at the 3rd Stokes in the backward direction was not measured because the dichroic mirror required to make the measurement reduced the incident pump power to below the threshold for the 3rd Stokes.

Using this approach, a slope efficiency of 88% for the combined Raman output energy (black triangles and solid line in Figure 3a) was measured for the microlens cavity, equating to 84% pump to combined Raman conversion efficiency at the highest pump pulse energy of 16µJ, seen in Figure 3a. A reduced conversion efficiency of 59% was measured in the plane-plane case, with a slope efficiency of 74% (black triangles and solid line in Figure 3b). The maximum average powers of the combined Raman outputs were 134mW and 96mW, respectively, for the micro-lens and plane-plane cases.

The Raman output in the microlens case had an M^2 of 6.8 x 4, 1.9 x 1.5 and 1.5 x 1.3 for the 1st, 2nd and 3rd

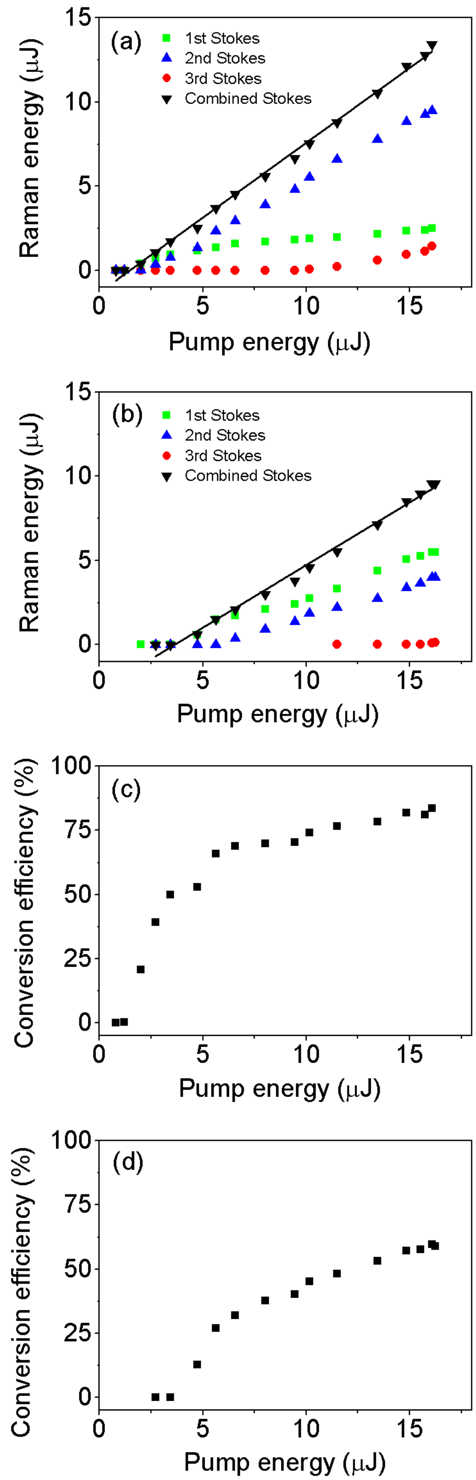

Figure 3. Energy transfer characteristics for the 1st (green squares) 2nd (blue triangles) and 3rd Stokes orders (red circles) and the combined Raman output (inverted black triangles) of (a) the microlens and (b) the plane-plane diamond Raman lasers, with (c) the conversion efficiency from pump to combined Raman in the microlens and (d) plane-plane cavities.

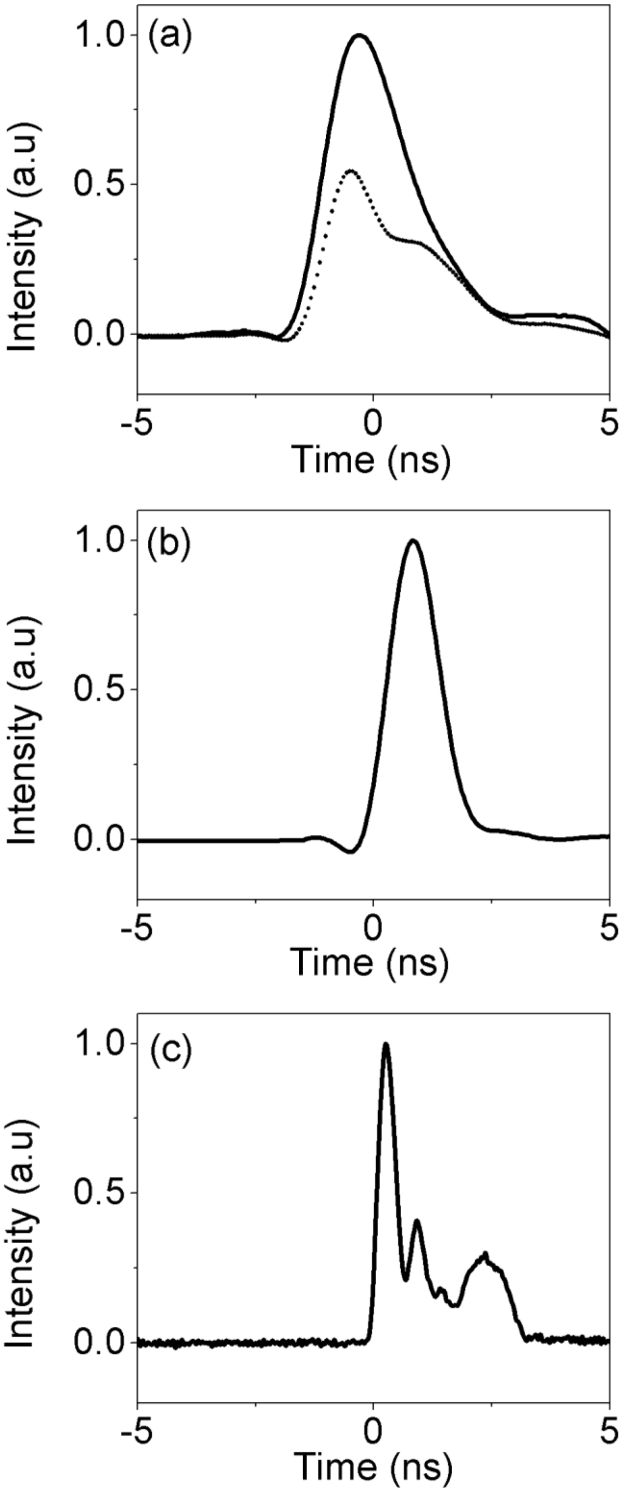

Figure 4. (a) Incident pump pulse (solid) compared with depleted pump pulse for the microlens case (dashed black), the measurement was taken at moderate pump powers. The 1st Stokes pulse at 573nm in the microlens case: (b) below the second Stokes threshold, and (c) at maximum pump energy with both 2nd and 3rd Stokes oscillating.

Stokes, respectively, at maximum pulse energy. The M^2 of the pump was 1.5 x 1.4. Issues with optical damage to the coatings made M^2 measurements difficult for the plane-plane case but values were no better than 3.6 x 3, 3.3 x 2.8 and 2.7 x 2.7 for the 1st, 2nd and 3rd Stokes respectively.

The 1st Stokes emission was polarized along a <110> direction in the diamond for both the microlens and plane-plane cavities, as would be expected from the polarization dependence of the Raman gain [3], [14]. No difference was observed in Raman output power when the microlens diamond was rotated for a pump polarization along a <111> direction. Although, in theory, orientating the pump along a <111> direction maximizes the Raman gain for propagation along <110> [3], [14], the Raman laser threshold is already small, so a significant change in Raman laser output power would not be expected.

Coating damage was observed much more readily on the plane-plane diamond than on the microlens crystal. Since the samples were coated in the same run, this might be indicative of poorer diamond surface quality in the plane-plane case.

The 1.5ns incident pump pulse is shown in Figure 4a (solid) along with the depleted pump (dashed). In the microlens and plane-plane cases, the 1st Stokes pulse duration (FWHM) was 1.2ns at low pump energies (below the threshold of the 2nd Stokes), as shown in Figure 4b. At maximum pump energy, however, depletion of the 1st Stokes by the 2nd Stokes, as shown in Figure 4c, meant the FWHM of the 1st Stokes pulse was not well defined. In the microlens case, the pulse duration of the 2nd Stokes was measured to be 1.6ns and the 3rd to be 0.9ns. Pulse durations of 1.1ns and 0.8ns for the 2nd and 3rd Stokes respectively were measured for the plane-plane device. Due to the significant conversion from 2nd to 3rd Stokes in the microlens cavity, it appears depletion has artificially increased the FWHM of the 2nd Stokes at maximum pump power.

The presence of three Stokes orders was confirmed using an Ocean Optics HR4000 spectrometer, with the spectrum shown in Figure 5. A spectrometer resolution of 0.13nm meant any sub-structure in the peaks was unresolved.

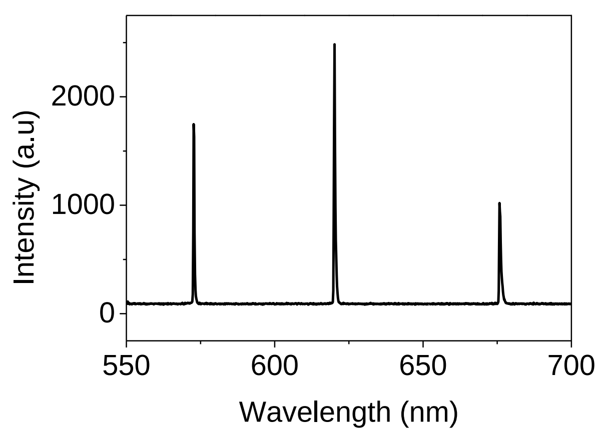

Figure 5. Typical spectral output in the microlens case showing the 1st Stokes at 573nm, 2nd Stokes at 620nm and 3rd Stokes at 676nm. Similar spectra were obtained in the plane-plane case.

The observation of Raman laser oscillation in the plane-plane case suggests that gain guiding [15] plays a role in transverse mode formation, since any thermal lens will be very weak. However, further experimental work is required to confirm this hypothesis and to elucidate any role gain-guiding might play in the microlens case.

A pronounced diffraction pattern is observed in the 1st Stokes output beam from the plane-plane cavity at high pump energies (see Figure 6a). This may be the result of interplay between the transverse mode and the spatially varying pump depletion and hence gain. In the case of the microlens cavity, the diffraction pattern is less pronounced (see Figure 6b), perhaps due to the microlens structure stabilising the transverse mode. A detailed analysis of these effects will be the subject of future work.

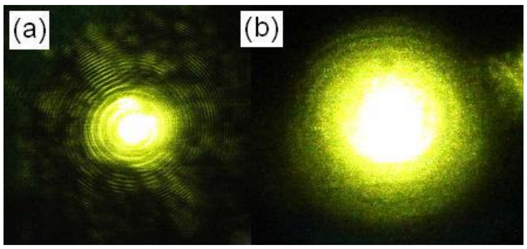

Figure 6. The 1st Stokes output beam at maximum pump pulse energy from the plane-plane (a) and micro-lens (b) cavities. (Not to scale.)

This demonstration highlights the ease with which emission at the 1st, 2nd and 3rd Stokes wavelengths can be generated in monolithic diamond Raman lasers. However, if only yellow output (573nm) is desired, the use of coatings with greater transmission for the higher Stokes orders is likely to improve the conversion efficiency to the yellow by eliminating cascaded Raman conversion. This may also improve the output beam quality at the 1st Stokes wavelength, which is currently being deteriorated by generation of higher Stokes components.

In conclusion, the feasibility of compact and robust monolithic diamond Raman lasers has been experimentally demonstrated. A conversion efficiency of 84% was achieved using microlens structures etched onto the front surface to form a stable cavity. In a simpler, plane-plane design, the Raman conversion efficiency was still 59%. Multiple Stokes orders were observed, and with further optimization of optical coatings, highly efficient laser action at any one of these wavelengths should be attainable.

The authors gratefully acknowledge funding from the European Research Council (DiaL: 278389), the UK Engineering and Physical Sciences Research Council (EPSRC; EP/I029141/1) and via a Fraunhofer UK / Royal Academy of Engineering Research Chair (AJK). SR and HL acknowledge an EPSRC DTA studentship and a China Scholarship Council studentship, respectively.

References

[1] I. Friel, S. L. Geoghegan, D. J. Twitchen, and G. A. Scarsbrook, *Proc. SPIE,* **7838**, 783819-1, (2010).

[2] V. G. Savitski, S. Reilly, and A. J. Kemp, *IEEE J. Quantum Electron.*, **49**, 218, (2013).

[3] V. G. Savitski, I. Friel, J. E. Hastie, M. D. Dawson, D. Burns, and A. J. Kemp, *IEEE J. Quantum Electron* , **48**, 328, (2012).

[4] O. Kitzler, A. McKay, and R. P. Mildren, *Opt. Lett.*, **37**, 2790, (2012).

[5] A. McKay, H. Liu, O. Kitzler, and R. P. Mildren, *Laser Phys. Lett.*, **10**, 105801, (2013).

[6] E. Granados, D. J. Spence, and R. P. Mildren, *Opt. Express*, **19**, 10857 (2011).

[7] J.-P. M. Feve, K. E. Shortoff, M. J. Bohn, and J. K. Brasseur, *Opt. Express*, **19**, 913 (2011).

[8] A. Sabella, J. a Piper, and R. P. Mildren, *Opt. Lett*, **39**, 4037 (2014).

[9] D. C. Parrotta, A. J. Kemp, M. D. Dawson, and J. E. Hastie, *Opt. Express*, **19**, 24165 (2011).

[10] F. A. L'Espernace, *Tr. Am. Opth. Soc*, **LXXXIII**, 82 (1985).

[11] J. R. F. De Abreu, *International Opthalmology*, **12,** 193 (1988).

[12] R. P. Mildren and A. Sabella, *Opt. Lett.*, **34**, 2811 (2009).

[13] H. W. Choi, E. Gu, C. Liu, C. Griffin, J. M. Girkin, I. M. Watson, and M. D. Dawson, *J. Vac. Sci. Technol. B Microelectron. Nanom. Struct.*, **23**, 130 (2005).

[14] A. Sabella, J. A. Piper, and R. P. Mildren, *Opt. Lett.*, **35**, 3874, (2010).

[15] F. Salin and J. Squier, *Opt. Lett.* **17**, 1352 (1992).

[1] I. Friel, S. L. Geoghegan, D. J. Twitchen, and G. A. Scarsbrook, “Development of high quality single crystal diamond for novel laser applications,” *Proc. SPIE*, vol. 7838, pp783819-1 - 783819-8, 2010.

[2] V. G. Savitski, S. Reilly, and A. J. Kemp, “Steady-State Raman Gain in Diamond as a Function of Pump Wavelength,” *IEEE J. Quantum Electron.*, vol. 49, no. 2, pp. 218–223, Feb. 2013.

[3] V. G. Savitski, I. Friel, J. E. Hastie, M. D. Dawson, D. Burns, and A. J. Kemp, “Characterization of Single-Crystal Synthetic Diamond for Multi-Watt Continuous-Wave Raman Lasers,” *IEEE JQE.*, vol. 48, no. 3, pp. 328–337, Mar. 2012.

[4] O. Kitzler, A. McKay, and R. P. Mildren, “Continuous-wave wavelength conversion for high-power applications using an external cavity diamond Raman laser,” *Opt. Lett.*, vol. 37, no. 14, pp. 2790–2792, Jul. 2012.

[5] A. McKay, H. Liu, O. Kitzler, and R. P. Mildren, “An efficient 14.5 W diamond Raman laser at high pulse repetition rate with first (1240 nm) and second (1485 nm) Stokes output,” *Laser Phys. Lett.*, vol. 10, no. 10, p. 105801, Oct. 2013.

[6] E. Granados, D. J. Spence, and R. P. Mildren, “Deep ultraviolet diamond Raman laser,” *Opt. Express*, vol. 19, no. 11, pp. 10857–10863, May 2011.

[7] J.-P. M. Feve, K. E. Shortoff, M. J. Bohn, and J. K. Brasseur, “High average power diamond Raman laser,” *Opt. Express*, vol. 19, no. 2, pp. 913–922, Jan. 2011.

[8] A. Sabella, J. a Piper, and R. P. Mildren, “Diamond Raman laser with continuously tunable output from 3.38 to 3.80 µm.,” *Opt. Lett.*, vol. 39, no. 13, pp. 4037–40, Jul. 2014.

[9] D. C. Parrotta, A. J. Kemp, M. D. Dawson, and J. E. Hastie, “Tunable continuous-wave diamond Raman laser,” *Opt. Express*, vol. 19, no. 24, pp. 24165–24170, Nov. 2011.

[10] F. A. L’Espernace, "Trans-spectral Organic Dye Laser photocoagulation", *Tr. Am. Opth. Soc*, vol. LXXXIII, 82, 1985.

[11] J. R. F. De Abreu, “The tunable dye laser in the management of retinal vascular disease”, *International Opthalmology*, vol. 196, pp. 193–196, 1988.

[12] R. P. Mildren and A. Sabella, “Highly efficient diamond Raman laser,” *Opt. Lett.*, vol. 34, no. 18, pp. 2811–2813, Sep. 2009.

[13] H. W. Choi, E. Gu, C. Liu, C. Griffin, J. M. Girkin, I. M. Watson, and M. D. Dawson, “Fabrication of natural diamond microlenses by plasma etching,” *J. Vac. Sci. Technol. B Microelectron. Nanom. Struct.*, vol. 23, no. 1, pp. 130, 2005.

[14] A. Sabella, J. A. Piper, and R. P. Mildren, “1240 nm diamond Raman laser operating near the quantum limit,” *Opt. Lett.*, vol. 35, no. 23, pp. 3874–3876, Dec. 2010.

[15] F. Salin and J. Squier, “Gain guiding in solid-state lasers”, *Opt. Lett*, vol. 17, no. 19, pp. 1352–1354, 1992.